

PROCEEDINGS OF SPIE

[SPIDigitalLibrary.org/conference-proceedings-of-spie](https://spiedigitallibrary.org/conference-proceedings-of-spie)

Porosity effects on red to far-red ratios of light transmitted in natural sands: implications for photoblastic seed germination

Gladimir V. G. Baranoski, Bradley W. Kimmel, Petri Varsa, Mark Iwanchyshyn

Gladimir V. G. Baranoski, Bradley W. Kimmel, Petri Varsa, Mark Iwanchyshyn, "Porosity effects on red to far-red ratios of light transmitted in natural sands: implications for photoblastic seed germination," Proc. SPIE 11149, Remote Sensing for Agriculture, Ecosystems, and Hydrology XXI, 111490O (21 October 2019); doi: 10.1117/12.2532495

SPIE.

Event: SPIE Remote Sensing, 2019, Strasbourg, France

Porosity Effects on Red to Far-Red Ratios of Light Transmitted in Natural Sands: Implications for Photoblastic Seed Germination

Gladimir V. G. Baranoski, Bradley W. Kimmel, Petri Varsa and Mark Iwanchyshyn

University of Waterloo, David R. Cheriton School of Computer Science, Natural Phenomena Simulation Group,
200 University Avenue West, Waterloo, Ontario, N2L 3G1, Canada

Abstract. Seed germination corresponds to the first and crucial stage of a plant's life cycle. It is directly affected by water availability and soil characteristics, notably porosity. The seeds of many plant species are known to be photoblastic, *i.e.*, their germination is also significantly affected by light exposure. A comprehensive understanding about the interconnected effects of these abiotic factors on seed germination is essential for the success of a broad range of applied research initiatives in agriculture and ecology. These initiatives include, for example, studies involving the germination of stress-adapted seeds in arid regions, like perennial desert habitats and desertified landscapes, and the germination of weed seeds in arable fields that may be covered by sand-textured soils (commonly referred to as natural sands). The germination of photoblastic seeds depends not only on the amount, but also on the spectral quality of the impinging light. This radiometric parameter can be expressed in terms of the ratio between red and far-red light reaching these seeds. In this research, we unveil the impact of variations in the porosity of sand-textured soils on their red to far-red ratios of transmitted light. Although one may expect that porosity can affect these ratios and, consequently, the germination of photoblastic seeds in natural sands, no systematic study about these putative connections has been reported in the literature to date. To some extent, this can be attributed to testing limitations posed by the actual handling of these granular materials, such as grain breakage and pore space disturbance, during investigations based on traditional experimental procedures. Moreover, the scant available information on these connections has been mostly derived from analyses performed on laboratory-prepared samples, which often present morphological characteristics that conspicuously differ from those of naturally-occurring deposits of these soils. In order to overcome these constraints, we employ an *in silico* investigation framework to carry out controlled light transmission experiments considering realistic characterizations of dry and water-saturated samples of natural sands. This framework is supported by measured spectral data and the use of a first-principles light transport model that explicitly accounts for the particulate structure of these materials. Our *in silico* experimental results provide a comprehensive depiction of the changes in the red to far-red ratios of light transmitted through natural sand layers of variable thickness due to variations on their porosity. Moreover, they also show that these changes are markedly modulated by the presence of water in these layers. Thus, our findings establish a predictive relationship between porosity and the light-elicited germination of photoblastic seeds in sand-textured soils subject to distinct degrees of water saturation. Accordingly, they are expected to contribute to the development of innovative technologies aimed at the predictive assessment (*in situ* or remote) of the compound impact of these abiotic factors on seed germination. These technologies, in turn, are likely to lead to new cost-effective solutions for ongoing challenges in agriculture (*e.g.*, crop yield enhancement) and ecology (*e.g.*, invasive plant detection and vegetation restoration), particularly with respect to regions susceptible to extreme environmental conditions.

Keywords: soil, sand, porosity, water saturation, transmittance, red to far-red ratio, germination, photoblastic seed.

1 INTRODUCTION

For decades, initiatives to increase crop yield while maintaining environmental stability have represented focal points of applied research programs in various fields, from plant physiology and agriculture to remote sensing and ecology, just to name a few. Recently, efforts to achieve these goals are being intensified by increasing global demands for food and biofuel production as well as adverse climate changes affecting natural resources, such as fresh water deposits, required to cope with these demands.

Two topics of permanent interest for these research programs are the invasion of weed seeds in arable fields and the cultivation of plant species more resilient to environmental stress.¹⁻⁴ While weed

invasion can be highly detrimental to farming, the cultivation of stress-adapted species can be substantially beneficial. Moreover, it has been observed that the more extreme the environment, the more efficient the mechanisms evolved by a plant in its overall adaptation to adverse growing conditions.³ Accordingly, plants capable of developing in perennial desert landscapes are also the object of investigations aimed at the restoration of vegetation in desertified ones.⁴ These arid landscapes are often characterized by a dominant presence of sand-textured soils, commonly referred to as natural sands. These soils are composed of a large amount of sand-sized grains (particles with dimensions between 0.05 to 2.0 *mm*) along with small amounts of silt-sized grains (particles with dimensions between 0.002 to 0.05 *mm*) and clay-sized grains (particles with dimensions smaller than 0.002 *mm*).⁵ Layers (of variable thickness) of natural sands can also be found covering arable fields. In addition, in some regions of the planet, they can be transported to farming areas by aeolian events (*e.g.*, sand storms⁶) originating from arid landscapes.

Seed germination, arguably the most fundamental stage in the life cycle of a plant,³ can be significantly affected by the mutual interactions of three crucial abiotic factors, namely water availability, light exposure and soil porosity. The latter is defined as the fraction of a soil's total volume occupied by its pore space (the volume not occupied by its constituent grains).⁷ In the case of natural sands, their porosity typically varies between 0.35 and 0.5,^{8,9} with values as low as 0.196^{9,10} and as high as 0.66^{9,11} being also reported in the literature.

The interactions between these abiotic factors are particularly exacerbated by tillage procedures used to prepare a soil for the cultivation of crops. These agricultural procedures affect the soil's structure,¹² increasing the size and proportion of its pore space. Since the porosity of a soil is inversely proportional to its compaction, tillage increases its porosity and reduces its compaction. A less compact (more porous) soil has a higher permeability and, consequently, higher water and air diffusivity.¹³ In addition, during tillage, a major portion of a seed bank receives light flashes that may be sufficient to stimulate germination.² Hence, an increase in porosity can positively affect the amount of water and light reaching buried seeds, with an increased volume fraction of the soil's pore space occupied by the former intensifying the transmission of the latter.^{1,2}

A large number of both dicot and monocot plant species are characterized by having photoblastic seeds, *i.e.*, seeds whose germination is influenced (positively or negatively) by light.¹⁴ This abiotic factor plays an important photomorphogenic role beneath the surface of sand-textured soils by affecting these seeds' germination timing.^{3,4,13,15,16} This, in turn, impacts the survival of resulting seedlings and the plants' fitness in subsequent life stages.^{4,14} These aspects further illustrate the relevance of the light exposure for seed germination, especially considering that photoblastic seeds are capable of responding to relatively small amounts of light and vast populations of them are found in arable soils.¹⁷

The germination of photoblastic seeds depends not only on the amount (photon flux density or PFD¹⁴), but also on the spectral quality of the light reaching them.^{2,14,16-19} While the former radiometric parameter affects the stimulation and inhibition of seed germination after long periods of light exposure, the latter affects these natural processes after both long and short periods of light exposure.¹⁴ Within this context, spectral quality can be expressed in terms of the ratio between red and far-red light reaching the seed.¹⁴

Clearly, a robust understanding about the effects of porosity variations on the spectral quality of light reaching photoblastic seeds is essential for the formulation of predictive models of weed emergence and cost-effective procedures for the cultivation of more resilient plant species.^{1,2} However, to

date, the available information on these effects, notably with respect to sand-textured soils subject to varying water saturation levels, remains relatively scant in the scientific literature. Relevant investigation efforts in related research areas usually employ lab-prepared sand samples,^{14,15,17,20} with experimental constraints often precluding the generalization of their outcomes to real scenarios involving natural sands.

These constraints can be loosely classified into three main varieties. The first corresponds to the absence of key morphological features of natural sands in soil samples artificially prepared in laboratory.^{21,22} These features include, for example, the complex size distribution patterns of their constituent grains (particles) within their pore space. The second variety encapsulates technical difficulties associated with the *in situ* assessment of the net effect of variations in multiple abiotic factors. For example, while attempting to place light sensors within a sample or changing its level of water saturation, one may inadvertently prompt situations (*e.g.*, grain breakage and interstitial space disturbance^{10,23}) that affect its porosity. Lastly, the third variety involves distortions caused by unnatural experimental conditions such as the use of dark rooms.¹⁸

In this paper, we employ an *in silico* experimental approach that allows us to overcome these constraints. Our goal is to provide a detailed assessment of the impact of porosity on the red to far-red ratios of light transmitted through dry and water-saturated layers of sand-textured soils. The focus of our investigation is on light that may reach shallowly buried seeds, *i.e.*, relatively low depths (less than 2 mm), which are known to be more relevant for the germination of photoblastic seeds found either in arable soils^{1,14} or arid landscapes.^{3,4,16}

Our *in silico* investigation approach consists in performing controlled experiments through predictive computer simulations supported by actual measured data. These experiments are carried out using a first-principles hyperspectral light transport model for particulate materials, known as SPLITS (*Spectral Light Transport Model for Sand*).²⁴ The model explicitly takes into account not only the specific mineralogical and morphological characteristics of the grains forming a sand sample, but also its porous structure. These aspects are particularly essential for studies examining the photobiological effects of light penetrating these soils.^{15,17}

It is worth noting that, for reproducibility purposes, we made SPLITS available for online use²⁵ via a model distribution system.²⁶ Through this system, researchers can specify experimental conditions (*e.g.*, angle of incidence and spectral range) as well as values for sand characterization parameters using a web interface,²⁵ and receive customized simulation results. Moreover, we also made the supporting data (*e.g.*, refractive index and extinction coefficient curves) used in our investigation available for online retrieval.²⁷

The remainder of this paper is organized as follows. In Section 2, we concisely review relevant biophysical concepts. In Section 3, we describe the *in silico* investigation framework employed in this research. In Section 4, we present our results and discuss their practical implications. Finally, in Section 5, we conclude the paper and outline directions for future work.

2 BIOPHYSICAL BACKGROUND

A wide range of plant species are characterized by the presence of proteins forming pigments, called phytochromes, that regulate various physiological and developmental processes. These processes include, for instance, seed germination, chloroplast movement, shade avoidance and photoperiodic time

measurement.^{14,28} The proteins of the phytochrome family of red to far-red light receptors, in particular, have demonstrated a diversity of spectral sensitivities and signaling mechanisms.²⁸ During exposure to light, they are constantly transformed from a red light absorbing conformation (denoted Pr) to a far-red light absorbing conformation (denoted Pfr), and back.^{19,28} In other words, absorption of red light by the Pr conformation converts the protein into the far-red light absorption Pfr conformation,²⁸ and vice-versa.

These two conformations can be thought as reversible red to far-red light-activated molecular switches.²⁸ The rate of cycling depends on the PFD and the spectral quality of the impinging light.¹⁴ Since the absorption spectra of Pr and Pfr overlap to some extent,²⁹ an equilibrium between Pr and Pfr can be established when they are exposed to light. Changes in the ratios of red to far-red impinging light can alter this equilibrium.²⁸ In most cases, physiological responses (*e.g.*, breaking of seed dormancy¹⁴) are induced by red light and cancelled by far-red light, leading to the idea that Pfr is the active conformation and Pr is the inactive one.¹⁴ Incidentally, as a counter-example, it is worth noting that experiments by Bell¹⁶ indicated that the germination of *Trachyandra divaricata* seeds, a sand dune inhabiting species found in Australia, was inhibited by red light.

In order to quantify the ratios of red to far-red light transmitted through soil that can eventually reach photoblastic seeds, researchers^{14,18} often use as sampling references the wavelengths that correspond to the absorption maxima of the chlorophyll Pr and Pfr phytochromes obtained under *in vitro* conditions, namely 660 and 730 *nm* respectively. Accordingly, we consider the following formula, henceforth denoted *in vitro* red to far-red ratio, to quantify the spectral quality of transmitted light in this investigation:

$$R/FR = \frac{\tau(660)}{\tau(730)}, \quad (1)$$

where $\tau(\lambda)$ denotes the transmittance at the wavelength λ (in *nm*).

It has been observed that chlorophyll competition for light under *in vivo* conditions shifts the Pr and Pfr phytochromes' action peaks to about 645 and 735 *nm*, respectively.¹⁹ Thus, for completeness, we also consider the following formula, henceforth denoted *in vivo* red to far-red ratio, to quantify the spectral quality of transmitted light in this investigation:

$$R^*/FR^* = \frac{\tau(645)}{\tau(735)}. \quad (2)$$

3 INVESTIGATION FRAMEWORK

Our *in silico* experiments primarily involve the computation of R/FR and R^*/FR^* ratios (Section 2) for two selected natural sand samples with distinct morphological and mineralogical characteristics. In order to compute these ratios using Eqs. 1 and 2, we have obtained directional-hemispherical transmittance curves for these samples using the SPLITS model. Prior to that, however, we have computed directional-hemispherical reflectance curves for these samples and compared them with measured ones. This step enabled us to assess the plausibility of the respective sample characterization datasets to be used in the computation of the transmittance curves.

It is worth stressing that SPLITS accounts for different iron-oxide distribution patterns within testing samples. Iron oxides, such as hematite and goethite, may occur as pure particles,³⁰ as contaminants mixed with the parent material,³¹ or as coatings, within a mineral matrix, formed on the grains during

wind transport.³² Normally, this matrix is composed of kaolinite and/or illite,³³ with the former (employed in this investigation) being more prevalent in natural sands.^{34,35} Also, in these soils, the parent (core) material is typically a material like quartz or calcite, with quartz (employed in this investigation) being the most common.³⁶

The measured reflectance curves used as references for the baseline modeled reflectance curves were made available in the U.S. Army Topographic Engineering Center (TEC) database.³⁷ They correspond to a sample from a dune in Saudi Arabia (TEC # 13j9823) and a sample from a dune in Australia (TEC # 10019201). Based on the descriptions of these samples,³⁷ we assumed that the presences of water and clay-sized particles were negligible.

For the computation of the baseline reflectance curves, besides considering a dry state ($S = 0$, where S represents the degree of water saturation), we employed average values for the porosity ($P = 0.425$), grain roundness ($R = 0.482$) and grain sphericity ($\Psi = 0.798$) found in the literature.^{8,38} The remaining model parameter values employed to characterize the selected natural sand samples are given in Table 1.

samples	sand	silt	pure grain	mixed grain	coated grain	r_{hg}	ϑ_{hg}
SD	85%	15%	10%	90%	0%	0.50	0.01
AD	85%	15%	0%	90%	10%	0.75	0.01

Table 1 Parameter values employed to characterize the Saudi Arabian dune (SD) and Australian dune (AD) samples considered in this investigation. The texture of the samples is described by the percentages of sand and silt. These percentages are used to compute the dimensions of the sand-sized particles (represented by spheroids whose major axis have on average a length equal to 0.236 mm) and the silt-sized particles (represented by spheroids whose major axis have on average a length equal to 0.045 mm) using a particle size distribution provided by Shirazi *et al.*³⁹ The particle type distributions employed in the simulations are given in terms of the percentages of pure, mixed and coated grains. The parameter r_{hg} corresponds to the ratio between the mass fraction of hematite to ϑ_{hg} (the total mass fraction of hematite and goethite).

Within the SPLITS' geometrical-optics formulation, light interacting with a given sand sample is represented by rays that can be associated with any wavelength. Hence, SPLITS can provide reflectance and transmittance curves with different spectral resolutions. For consistency, all modeled curves depicted in this work cover the spectral region of interest from 600 to 800 nm (containing the wavelengths employed in the computation of the R/FR and R^*/FR^* as defined in Section 2) and have a spectral resolution of 5 nm. These curves were obtained using a virtual spectrophotometer.⁴⁰ In their computation, we considered 10^6 sample rays (per sampled wavelength) to obtain asymptotically convergent readings,⁴⁰ and an angle of incidence of 0° for consistency with the actual experimental set-up employed by Rinker *et al.*^{24,37} to obtain the reference measured reflectance curves.

The reflectance of sand samples rapidly reaches a plateau (occasionally referred to as “infinite reflectance”) as one considers increasing sample thickness (depth) values.⁴¹ In the case of natural sand samples characterized by the presence of strong light absorbers (*e.g.*, iron oxides), this plateau is reached when one considers thickness values on the order of millimeters.²¹ Consequently, the reflectance of natural sand deposits is guaranteed to reach this plateau since these deposits normally have fairly large depths, on the order of meters. Thus, without loss of generality, we consider a sample thickness of 1 m in the computation of the baseline reflectance curves presented in Fig. 1.

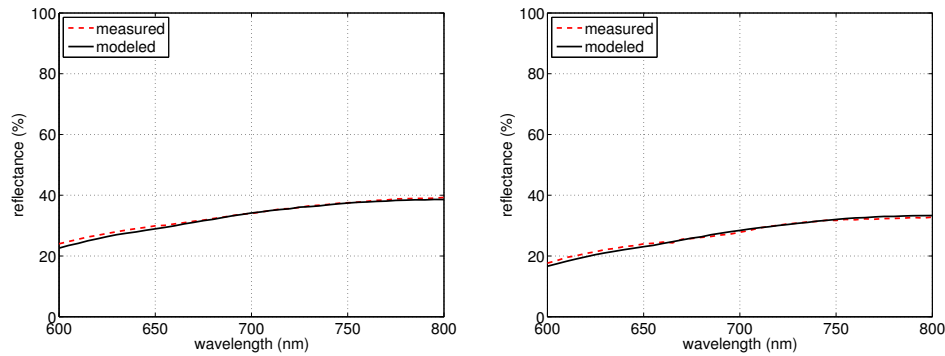


Fig 1 Comparisons of measured³⁷ and modeled reflectance curves for the Saudi Arabian dune sample (left) and the Australian dune sample (right).

As it can be observed in the graphs depicted in Fig. 1, the baseline modeled reflectance curves computed for the two selected natural sand samples show a close agreement with their measured references. Accordingly, we also employed the characterization datasets provided in Table 1 to obtain the transmittance curves resulting from variations in the samples, porosity (P from 0.2 to 0.7) when they are subjected to dry ($S = 0$) and water-saturated ($S = 1$) states.

Finally, for the computation of the transmittance curves, we selected sample thickness values equal to 1.0 and 1.5 mm. These values correspond to standard light penetration depths considered in agricultural and ecological investigations.^{1-3,22} Moreover, we note that the transmittance of natural sand samples rapidly tends to zero as one considers increasing values for their thickness.⁴¹ Thus, the selected thickness values allow for the computation of R/FR and R^*/FR^* ratios less affected by errors that may follow mathematical operations involving exceedingly small numbers (represented by small transmittance values in this context)

4 RESULTS AND DISCUSSION

In our first set of *in silico* experiments, we computed the transmittances for the selected samples considering an average value for their porosity ($P = 0.425$) and two water saturation states ($S = 0$ and $S = 1$). As it can be observed in the graphs depicted in Fig. 2, an increase in thickness is followed by a significant decrease in transmittance. Moreover, one can also observe that an increase in the degree of water saturation is followed by an increase in transmittance. We note that both trends have been detected in spectrophotometric measurements reported in the literature.^{1,2,22,41} This qualitative consistency between our observations and actual measured data strengthened our confidence in the predictive capabilities of our *in silico* experimental framework. It also provided a solid foundation for our subsequent experiments.

In Tables 2 and 3, we present the values for R/FR and R^*/FR^* ratios calculated using the corresponding transmittance values extracted from the curves depicted in Fig. 2. Upon inspection of these values, one can note that both ratios decrease as the samples' thickness increases, and decrease as the degree of water saturation increases. It is worth noting that these trends have also been observed in previous radiometric experiments,¹⁵ with the changes in the red to far-red ratios being attributed to spectral shifts in the transmittance spectra due to variations in the samples' thickness and degree of

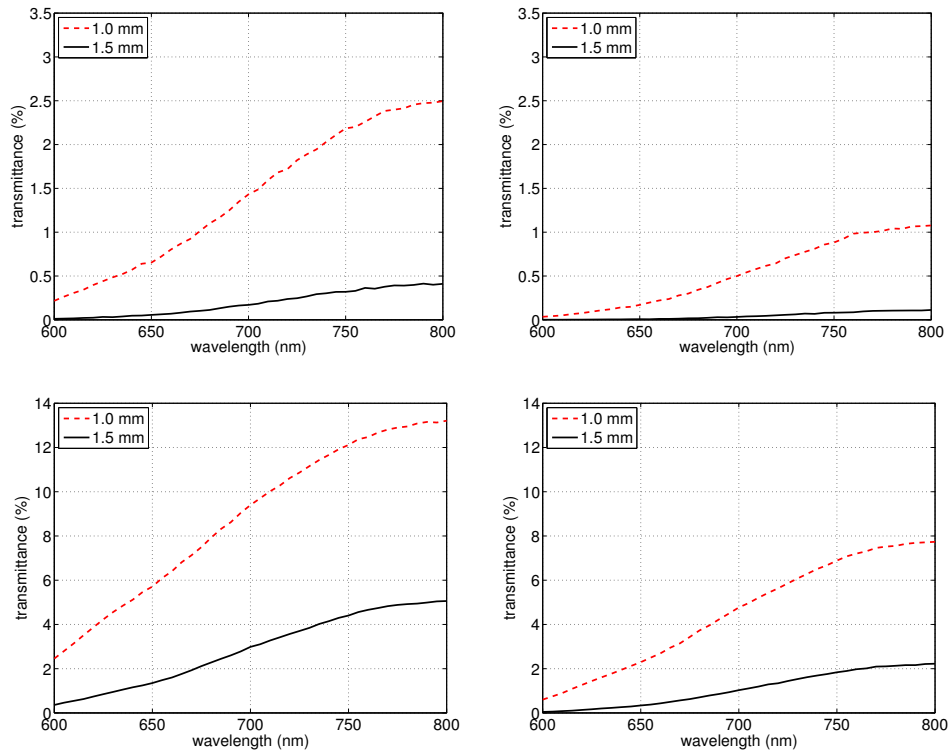


Fig 2 Comparisons of modeled transmittance curves computed for the Saudi Arabian dune sample (left column) and the Australian sample (right column). These curves were obtained employing an average value for their porosity ($P = 0.425$) and two values for their thickness (1.0 and 1.5 mm). In addition, we also considered two values for their degree of water saturation (S). Top row: $S = 0$. Bottom row: $S = 1$.

water saturation. Finally, the values obtained for the R^*/FR^* ratios are consistently lower than those obtained for the R/FR ratios. This trend, in turn, can be explained by the fact that the transmittance values used in the calculation of these ratios are characterized by a monotonic increase from 645 to 660 nm.

In our second set of *in silico* experiments, we have computed the transmittance curves of the selected samples considering variations in their porosity (P from 0.2 to 0.7) and degree of water saturation ($S = 0$ and $S = 1$). For illustrative purposes, we present in Fig. 3 the graphs depicting

thickness	SD		AD	
	$S = 0$	$S = 1$	$S = 0$	$S = 1$
1.0 mm	0.4239	0.5742	0.2980	0.4425
1.5 mm	0.2594	0.4170	0.1715	0.2818

Table 2 Values calculated for the *in vitro* red to far-red ratios (R/FR) using transmittance readings obtained at 660 nm and 730 nm for the selected Saudi Arabian dune (SD) and Australian dune (AD) samples, whose corresponding transmittance curves are depicted in Fig. 2. These curves were obtained considering distinct values for the samples' degree of water saturation (S).

thickness	SD		AD	
	$S = 0$	$S = 1$	$S = 0$	$S = 1$
1.0 mm	0.3286	0.4780	0.1911	0.3370
1.5 mm	0.1684	0.3092	0.0875	0.1799

Table 3 Values calculated for the *in vitro* red to far-red ratios (R^*/FR^*) using transmittance readings obtained at 645 nm and 735 nm for the selected Saudi Arabian dune (SD) and Australian dune (AD) samples, whose corresponding transmittance curves are depicted in Fig. 2. These curves were obtained considering distinct values for the samples' degree of water saturation (S).

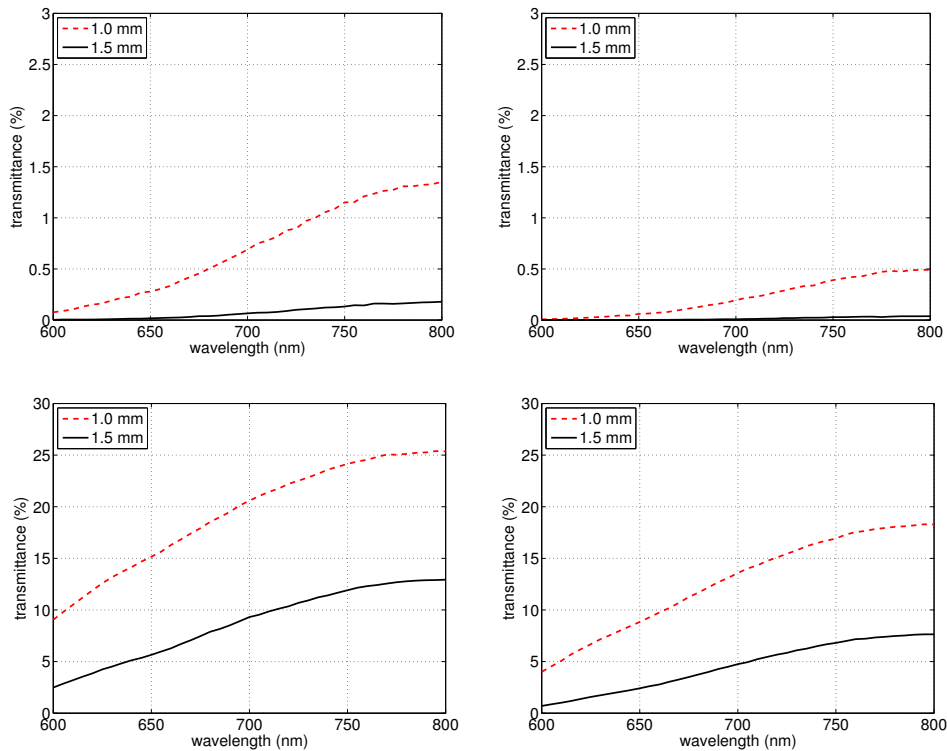


Fig 3 Comparisons of modeled transmittance curves computed for the Saudi Arabian dune sample (left column) and the Australian sample (right column) considering distinct values for their thickness (1.0 and 1.5 mm). These curves were obtained employing lower and upper bounds for their porosity (P) and degree of water saturation (S). Top row: $P = 0.2$ and $S = 0$. Bottom row: $P = 0.7$ and $S = 1$.

the curves associated with the lower ($P = 0.2$ and $S = 0$) and upper ($P = 0.7$ and $S = 1$) bounds for these parameters. One can observe in these curves the transmittance behaviours highlighted before (Fig. 2). The same can be stated for their corresponding R/FR (Table 4) and R^*/FR^* (Table 5) ratios, which show the same trends pointed out for the R/FR and R^*/FR^* ratios presented in Tables 2 and 3, respectively.

The full range of changes in the R/FR and R^*/FR^* ratios associated with the transmittance values computed considering the specified variations in their porosity (P from 0.2 to 0.7) and degree of water

thickness	SD		AD	
	$P = 0.2 \ \& \ S = 0$	$P = 0.7 \ \& \ S = 1$	$P = 0.2 \ \& \ S = 0$	$P = 0.7 \ \& \ S = 1$
1.0 mm	0.3435	0.7131	0.2311	0.6181
1.5 mm	0.2171	0.5747	0.1161	0.4560

Table 4 Values calculated for the *in vitro* red to far-red ratios (R/FR) using transmittance readings obtained at 660 nm and 730 nm for the selected Saudi Arabian dune (SD) and Australian dune (AD) samples, whose corresponding transmittance curves are depicted in Fig. 3. These curves were obtained considering lower and upper bounds for the samples' porosity (P) and degree of water saturation (S).

thickness	SD		AD	
	$P = 0.2 \ \& \ S = 0$	$P = 0.7 \ \& \ S = 1$	$P = 0.2 \ \& \ S = 0$	$P = 0.7 \ \& \ S = 1$
1.0 mm	0.2671	0.6334	0.1332	0.5206
1.5 mm	0.1249	0.4780	0.0342	0.3555

Table 5 Values calculated for the *in vitro* red to far-red ratios (R^*/FR^*) using transmittance readings obtained at 645 nm and 735 nm for the selected Saudi Arabian dune (SD) and Australian dune (AD) samples, whose corresponding transmittance curves are depicted in Fig. 3. These curves were obtained considering lower and upper bounds for the samples' porosity (P) and degree of water saturation (S).

saturation ($S = 0$ and $S = 1$) are depicted in the graphs presented in Figs. 4 and 5, respectively. As it can be observed in these graphs, an increase in the samples' porosity is followed by an increase in both ratios. We note that this trend is more accentuated for higher porosity values.

It has been recognized that the presence of water in the soil can strongly affect the responses of photoblastic seeds to light, with high red to far-red ratios being often required to break the dormancy of seeds buried in soils characterized by a low degree of water saturation.¹³ Our *in silico* experiments indicate that an increase in porosity can increase the red to far-red ratios of light transmitted through sand-textured soils. Hence, by increasing the porosity of these soils, one may be able to reduce the negative effects of a low water content. This corroborates previous postulations on the positive effects of high porosity (low compaction) on the germination of photoblastic seeds.¹³

We note that man-managed (*e.g.*, tillage) or environmental (*e.g.*, wind) processes can contribute to an increase in the porosity of sand-textured soils. Consequently, these processes can also affect the germination of photoblastic seeds buried in these soils. Thus, their potential impact on pressing agricultural and ecological concerns, like the reduction of weed invasion in arable fields and the restoration of vegetation in desertified landscapes, should be closely examined.

Finally, we remark that the transmittance of natural sands in the spectral region of interest, from 600 to 800 nm, is directly associated with the absorption spectra of iron oxides found in these soils. Thus, as it has been demonstrated by the results obtained for the two distinct samples considered in our investigation, spectral shifts affecting the transmittance and, consequently, the red to far-red ratio of light penetrating these soils, are also connected to the contents of these minerals present in a given sample. For example, the red to far-red ratios computed for the Saudi Arabian dune sample were higher than those computed for the Australian dune sample. Recall that the former is characterized by

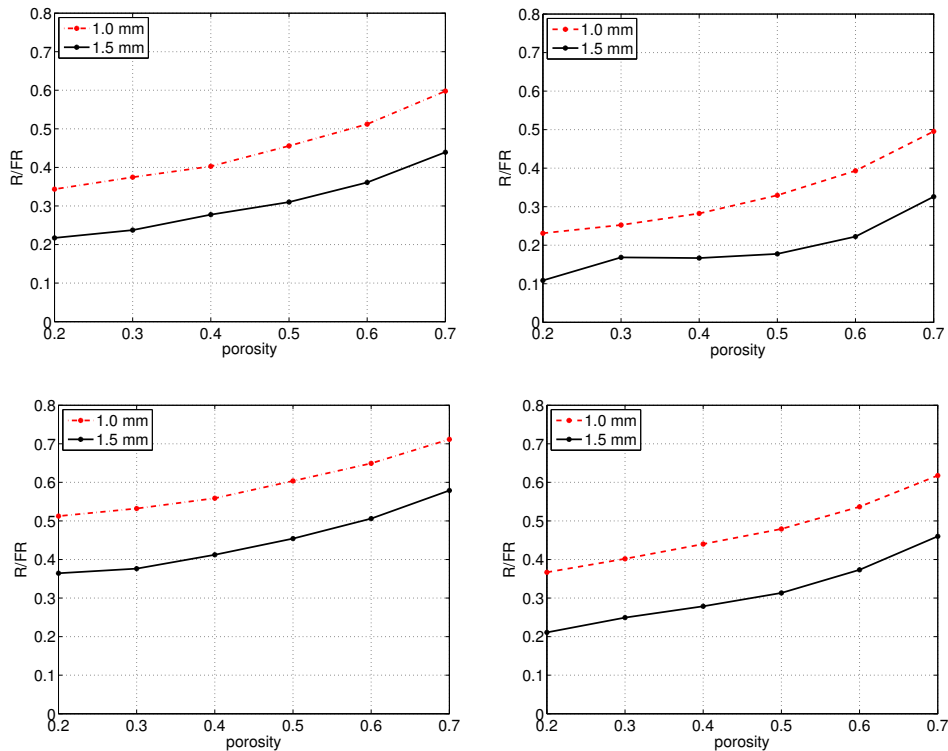


Fig 4 Comparisons of *in vitro* red to far-red ratios (R/FR) values calculated using transmittance readings computed at 660 nm and 730 nm for the selected Saudi Arabian dune sample (left column) and the selected Australian sample (right column). These readings were obtained considering distinct values for the samples' thickness (1.0 and 1.5 mm), porosity and degree of water saturation (S). Top row: $S = 0$. Bottom row: $S = 1$.

a lower iron oxide content, which leads to the steeper incline observed in its transmittance curves in the spectral region of interest. Therefore, one has to take these mineralogical aspects into account in the quantitative generalization of our findings.

5 Conclusion and Future Work

In the last decades, researchers from different disciplines have been examining how seed germination can be affected by water availability and light exposure, notably with respect to the red to far-red ratio of impinging light. Relevant research efforts have also been directed toward the effects of soil porosity on light transmission. To date, however, only scant information can be found about the impact of porosity variations on the red to far-red ratios of light transmitted through natural sands. This may be largely attributed to practical difficulties in properly accounting for the actual morphological and mineralogical characteristics of these soils while performing light transmission experiments on them. To overcome these constraints, we employed an *in silico* investigation approach in the research described in this paper. It enabled us to demonstrate the sensitivity of these ratios to variations on the porosity of distinct natural sand samples subject to different water saturation states. Our findings indicate that the negative effects of low red to far-red ratios on the germination of seeds of many species positively susceptible to light exposure, particularly considering limited water availability, can

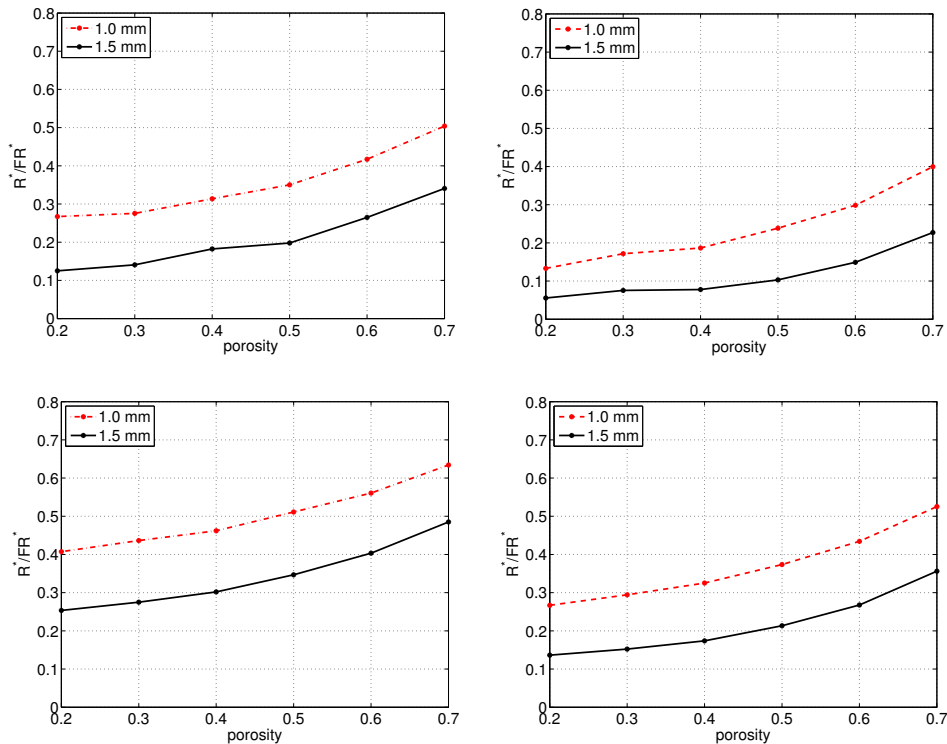


Fig 5 Comparisons of *in vivo* red to far-red ratios (R^*/FR^*) values calculated using transmittance readings computed at 645 nm and 735 nm for the selected Saudi Arabian dune sample (left column) and the selected Australian sample (right column). These readings were obtained considering distinct values for the samples' thickness, porosity and degree of water saturation (S). Top row: $S = 0$. Bottom row: $S = 1$.

be mitigated by processes leading to an increase in the porosity of the target sand-textured soils. More broadly, the results of our investigation strengthen the knowledge basis required for the predictive assessment (*in situ* or remote) of abiotic factors affecting the germination of seeds in sand-textured soils. Such an assessment, in turn, can be instrumental in the search for effective solutions for open problems in agriculture and ecology.

In the research described in this paper, we considered natural sand samples subject to dry and water-saturated states. As future work, we intend to increase the testing resolution of our *in silico* experiments with respect to the samples' degree of water saturation. More specifically, by incrementally varying this parameter, we plan to investigate the behaviour (*e.g.*, linear, quadratic or exponential) of the resulting increase in the red to far-red ratios. In addition, we plan to extend our scope of observations to dry layers of natural sands whose grains, albeit immersed in a pore space filled with air, are enveloped by water films of variable thickness. In other words, layers whose pore space has previously been occupied and/or traversed by water, which has either percolated to underneath layers or partially evaporated, leaving only the water films around the grains. Finally, we note that grain shape can vary considerably depending on the transportation processes (*e.g.*, by water or wind) leading to the formation of natural sand deposits. For example, water-transported grains tend to have smoother surfaces than wind-transported grains, whose sphericity tends to increase as the last stage of aeolian transportation becomes harsher.⁴² Thus, in our future work, we also plan to closely examine the effects

of variations of sand grain shape on the red to far-red ratios of light transmitted through natural sand layers of variable thickness and subject to different water saturation states.

Acknowledgments

This work was supported by the Natural Sciences and Engineering Research Council of Canada (NSERC-Discovery Grant 238337).

References

- 1 J. Woolley and E. Stoller, "Light penetration and light-induced seed germination in soil," *Plant Physiol.* **61**, pp. 597–600, 1978.
- 2 S. Benvenuti, "Soil light penetration and dormancy of Jimsonweed (*Datura stramonium*) seeds," *Weed Sci.* **43**, pp. 389–393, 1995.
- 3 D. Koller, M. Sachs, and M. Negbi, "Germination-regulation mechanisms in some desert seeds VIII *Artemisia monosperma*," *Plant Cell Physiol.* **5**, pp. 85–100, 1964.
- 4 L. Lai, L. Chen, L. Jiang, J. Zhou, Y. Zheng, and H. Shimizu, "Seed germination of seven desert plants and implications for vegetation restoration," *AoB Plants* **8**, pp. 1–10, 2016.
- 5 Soil Science Division Staff, "Soil survey manual," Tech. Rep. USDA Handbook 18, Soil Conservation Service, United States Department of Agriculture, 1993.
- 6 M. Akhlaq, T. Sheltami, and H. Mouftah, "A review of techniques and technologies for sand and dust storm detection," *Rev. environ. Sci. Biotechnol.* **11**, pp. 305–322, 2012.
- 7 N. Brady and R. Weil, *Elements of the Nature and Properties of Soils*, Prentice-Hall Inc., Upper Saddle River, NJ, USA, 2000.
- 8 N. Brady, *The Nature and Properties of Soils*, Macmillan Publishing Co., New York, NY, USA, 8th ed., 1974.
- 9 J. Román-Sierra, J. Muñoz-Perez, and M. Navarro-Plus, "Beach nourishment effects on sand porosity variability," *Coast. Eng.* **83**, pp. 221–232, 2014.
- 10 W. Dickinson and J. Ward, "Low depositional porosity in eolian sands and sandstones, Namib desert," *J. Sediment. Res.* **A64**(2), pp. 226–232, 1994.
- 11 P. Jackson, D. Smith, and P. Stanford, "Resistivity-porosity-particle shape relationships for marine sands," *Geophysics* **43**, pp. 1250–1268, 1978.
- 12 J. Lipiec, J. Kuś, A. Slowińska-Jurkiewicz, and A. Nosalewicz, "Soil porosity and water infiltration as influenced by tillage methods," *Soil Till Res.* **89**, pp. 210–220, 2016.
- 13 M. Bejarano, R. Villar, A. Murillo, and J. Quero, "Effects of soil compaction and light on the growth of *Quercus pyrenaica* Willd. (*Fagaceae*) seedlings," *Soil Till Res.* **110**, pp. 108–114, 2010.
- 14 T. Pons, "Seed responses to light," in *Seeds: The Ecology of Regeneration in Plant Communities*, M. Fenner, ed., pp. 237–260, CABI Publishing, (Wallingford, UK), 2000.
- 15 D. Mandoli, G. Ford, L. Waldron, J. Nemson, and W. Briggs, "Some spectral properties of several soil types: implications for photomorphogenesis," *Plant Cell Environ.* **13**, pp. 287–294, 1990.
- 16 D. Bell, "The effect of light quality on the germination of eight species from sandy habitats in Western Australia," *Aust. J. Bot.* **41**(3), pp. 321–326, 1993.
- 17 D. Bliss and H. Smith, "Penetration of light into soil and its role in the control of seed germination," *Plant Cell Environ.* **8**, pp. 475–483, 1985.

- 18 H. Smith, "Light quality, photoperception, and plant strategy," *Ann. Rev. Plant Physiol.* **33**, pp. 481–518, 1982.
- 19 M. Kasperbauer, "Far-red light reflection from green leaves and effects on phytochrome-mediated assimilate partitioning under field conditions," *Plant Physiol.* **85**, pp. 350–354, 1987.
- 20 M. Kasperbauer and P. Hunt, "Biological and photometric measurement of light transmission through soils of various colors," *Bot. Gaz.* **149**(4), pp. 361–364, 1988.
- 21 D. Bänninger and H. Flühler, "Modeling light scattering at soil surfaces," *IEEE T. Geosci. Remote* **42**(7), pp. 1462–1471, 2004.
- 22 M. Tester and C. Morris, "The penetration of light through soil," *Plant Cell Environ.* **10**, pp. 281–286, 1987.
- 23 D. Tang, K. Briggs, K. Williams, D. Jackson, E. Thorsos, and D. Percival, "Fine-scale volume heterogeneity measurements in sand," *Soil Sci. Soc. Am. J.* **27**(3), pp. 546–560, 2002.
- 24 B. Kimmel and G. Baranoski, "A novel approach for simulating light interaction with particulate materials: application to the modeling of sand spectral properties," *Opt. Express* **15**(15), pp. 9755–9777, 2007.
- 25 Natural Phenomena Simulation Group (NPSG), *Run SPLITS Online*. David R. Cheriton School of Computer Science, University of Waterloo, Ontario, Canada, 2012. <http://www.npsg.uwaterloo.ca/models/splits.php>.
- 26 G. Baranoski, T. Dimson, T. Chen, B. Kimmel, D. Yim, and E. Miranda, "Rapid dissemination of light transport models on the web," *IEEE Comput. Graph.* **32**(3), pp. 10–15, 2012.
- 27 Natural Phenomena Simulation Group (NPSG), *Sand Data*. David R. Cheriton School of Computer Science, University of Waterloo, Ontario, Canada, 2012. <http://www.npsg.uwaterloo.ca/data/sand.php>.
- 28 R. Sharrock, "The phytochrome red/far-red photoreceptor superfamily," *Genome Biol.* **9**(8), pp. 230:1–7, 2008.
- 29 C. Fankhauser, "The phytochromes, a family of Red/Far-red absorbing photoreceptors," *J. Biol. Chem.* **276**(15), pp. 11453–11456, 2001.
- 30 D. Catling and J. Moore, "The nature of coarse-grained crystalline hematite and its implications for the early environment of Mars," *Icarus* **165**, pp. 277–300, 2003.
- 31 A. Mottana, R. Crespi, and G. Liborio, *Simon and Schuster's Guide to Rocks and Minerals*, Simon and Schuster, Inc., New York, NY, USA, 1978.
- 32 H. Wopfner and C. Twidale, "Australian desert dunes: wind rift or depositional origin?," *Aust. J. Earth Sci.* **48**, pp. 239–244, 2001.
- 33 H. Wopfner and C. Twidale, "Formation and age of desert dunes in Lake Eyre depocentres in central Australia," *Geologische Rundschau* **77**(3), pp. 815–834, 1988.
- 34 F. El-Baz and D. Prestel, "Coatings on sand grains from Southwestern Egypt," in *Desert Landforms of Southwest Egypt: A Basis for Comparison with Mars (NASA CR-3611)*, F. El-Baz and T. Maxwell, eds., pp. 175–188, National Air and Space Museum Smithsonian Institution and National Aeronautics and Space Administration (NASA), (Washington, DC, USA), 1982. Chapter 13.

- 35 R. Rossel, E. Bui, P. de Caritat, and N. McKenzie, "Mapping iron oxides and the color of Australian soil using visible-near-infrared reflectance spectra," *J. Geophys. Res.* **115**, pp. F04031–1–13, 2010.
- 36 D. Leu, "Visible and near-infrared reflectance of beach sands: a study on the spectral reflectance/grain size relationship," *Remote Sens. Environ.* **6**(3), pp. 169–182, 1977.
- 37 J. Rinker, C. Breed, J. McCauley, and P. Corl, "Remote sensing field guide – desert," Tech. Rep. ETL-0588, U.S. Army Topographic Engineering Center, Fort Belvoir, VA, USA, September 1991.
- 38 M. Vepraskas and D. Cassel, "Sphericity and roundness of sand in coastal plain soils and relationships with soil physical properties," *Soil Sci. Soc. Am. J.* **51**(5), pp. 1108–1112, 1987.
- 39 M. Shirazi, L. Boersma, and J. Hart, "A unifying quantitative analysis of soil texture: Improvement of precision and extension of scale," *Soil Sci. Soc. Am. J.* **52**(1), pp. 181–190, 1988.
- 40 G. Baranoski, J. Rokne, and G. Xu, "Virtual spectrophotometric measurements for biologically and physically-based rendering," *Visual Comput.* **17**(8), pp. 506–518, 2001.
- 41 A. Ciani, K. Goss, and R. Schwarzenbach, "Light penetration in soil and particulate materials," *Eur. J. Soil. Sci.* **56**, pp. 561–574, 2005.
- 42 G. Baranoski, B. Kimmel, T. Chen, and E. Miranda, "Influence of sand-grain morphology and iron-oxide distribution patterns on the reflectance of sand-textured soils," *IEEE J-STARS* **7**(9), pp. 3755–3763, 2014.